

Thermal Activation Pathways in HEA Stabilized Quantum Emitters

Ashwani Kumar^{1*}

Department of Physics, National Defence Academy, Kadakwasla, Pune – 411023, Maharashtra

***Correspondence:**

Ashwani Kumar

Department of Physics, National Defence Academy, Kadakwasla, Pune – 411023, Maharashtra.

Received: May 25, 2026;**Published:** June 15, 2026**How to cite this article:**A. Kumar, "Thermal Activation Pathways in HEA Stabilized Quantum Emitters," *Phys. J. Theor. Exp. Stud.* 2(2), 1–7 (2026). <https://doi.org/10.64978/pjtes.2026.0615009>**Abstract**

High entropy alloy (HEA) engineering offers a powerful route to stabilize semiconductor quantum dots (QDs) under harsh thermal and photonic environments. In this work, we develop a unified quantum mechanical and empirical framework to elucidate the thermal activation behavior of CdSe–HEA QDs. Quantum level modeling shows that multielement HEA interfaces introduce distributed electronic states, suppress surface traps, and enhance radiative exciton recombination by modifying the local potential landscape of the CdSe core. To quantify the resulting stability, we employ an Arrhenius based degradation formalism, treating photoluminescence (PL) decay as a first order thermally activated process. The HEA modified QDs exhibit a significantly higher activation energy (0.90 eV) compared to bare CdSe (0.60 eV), leading to an exponential increase in emissive lifetime. Empirical predictions reveal a 10^3 – 10^4 fold lifetime enhancement across 350–500 K and sustained PL retention ($S > 0.95$) up to ~480 K, extending the operational temperature window by nearly 100 K. Composite analyses including Arrhenius plots, stability maps, and lifetime enhancement curves demonstrate that configurational entropy stabilization in the HEA shell effectively suppresses nonradiative pathways and thermal degradation. These results establish CdSe–HEA QDs as robust, entropy stabilized nanomaterials with strong potential for high temperature optoelectronic, photocatalytic, and energy conversion applications.

Keywords: CdSe quantum dots; High entropy alloys; Thermal stability; Arrhenius kinetics; Exciton dynamics; Lifetime enhancement**1. Introduction**

Quantum dots (QDs) have evolved into one of the most versatile classes of nanoscale semiconductors due to their discrete energy levels, strong quantum confinement, and size dependent optical and electronic properties. The foundational work of Murray, Norris, and Bawendi in 1993 established reliable synthetic routes for nearly monodisperse II–VI nanocrystals, including CdSe, CdS, and CdTe, thereby enabling systematic exploration of their structure–property relationships.¹ Since then, CdSe QDs have become a model system for optoelectronic and photonic applications owing to their tunable bandgap, high photoluminescence quantum yield (PLQY), and narrow emission linewidths.

Advances in synthetic chemistry have further expanded the capabilities of CdSe QDs. Green and phosphine free synthesis routes now allow precise control over particle size, crystallinity, and optical purity, as demonstrated by Bamanian, Gupta, and Manisha, who achieved high quality CdSe QDs with narrow PL full width at half maximum (FWHM) and excellent colloidal stability.² Beyond optical applications, CdSe QDs have recently gained prominence in electrochemical energy storage. Kazemi and co workers showed that CdSe QDs enhance charge storage, cycling stability, and pseudocapacitive behavior in lithium ion batteries and supercapacitors due to their high surface area, tunable band structure, and efficient charge transfer pathways.³ Alloyed systems such as CdSeTe QDs have also been developed to achieve color tunable emission and improved PLQY, with Elibol, Demirci, and Koç demonstrating optimized green and red emission through controlled precursor ratios and chloride passivation.⁴

In parallel, CdSe QDs have emerged as promising candidates for nonlinear optical applications. Jain, Maikhuri, and Sahai reported efficient difference frequency generation (DFG) in CdSe QDs, attributing the enhanced second order susceptibility to strong confinement

induced intersubband transitions.⁵ Their subsequent work on CdSe/ZnS, CdSe/ZnSe, CdSe/MgS, and CdSe/MgSe heterostructures revealed that shell composition and band offsets significantly influence second order nonlinear susceptibility, offering new pathways for mid infrared photonics and quantum optical devices.⁶ More recently, Noh, Livache, Hahm, Pinchetti, Jin, Kim, and Klimov demonstrated highly efficient carrier multiplication in inverted CdSe/HgSe QDs mediated by magnetic impurities, highlighting the potential of engineered electronic landscapes to enhance hot carrier utilization.¹²

While CdSe based QDs have matured significantly, a parallel revolution has unfolded in the field of high entropy alloys (HEAs). Introduced independently by Yeh and co workers⁷ and by Cantor and colleagues,⁸ HEAs incorporate five or more principal elements in near equiatomic ratios, stabilizing single phase solid solutions through high configurational entropy. HEAs exhibit unique “cocktail effects,” sluggish diffusion, and enhanced thermodynamic stability, enabling exceptional mechanical, catalytic, and electronic properties. Recent advances in ultra high entropy alloy nanoparticles (HEANPs), as reviewed by Mahin, Kusada, and Kitagawa, demonstrate that nanoscale HEAs can incorporate six or more elements while retaining structural homogeneity and tunable electronic behavior.⁹

The extension of HEA concepts into semiconductor nanocrystals has produced remarkable results. Chiang, Shivarudraiah, Wieczorek, Khoo, Leong, Lim, Xing, Kumar, Solari, Li, Chiu, Sum, Liu, Siol, and Shih synthesized high entropy alloyed perovskite nanocrystals and showed that multi cation incorporation at the B site reduces band dispersion, introduces shallow states, and enhances photostability and radiative recombination.¹⁰ Similarly, Zhao, Guo, Tang, Zhu, Xie, Li, Shao, Xu, Wang, and Lu demonstrated that rare earth based high entropy halide perovskite QDs exhibit outstanding environmental stability, retaining over 70% of their PL intensity after 60 days and maintaining strong luminescence under thermal and chemical stress.¹¹

Despite these breakthroughs, no study has yet explored the integration of high entropy alloy principles with classical II–VI semiconductor quantum dots such as CdSe. This gap is scientifically significant for several reasons:

- CdSe QDs possess well defined excitonic physics but face limitations in thermal stability, defect tolerance, and band structure tunability.
- HEA nanocrystals exhibit entropy driven stabilization, shallow state formation, and electronic tunability, but these effects have only been demonstrated in metallic, oxide, sulfide, and halide perovskite systems not in II–VI semiconductors.
- No theoretical or experimental framework exists for multi cation substitution at the Cd site or Se site in CdSe QDs.
- The potential synergy between HEA induced electronic disorder and CdSe quantum confinement remains unexplored, despite evidence that engineered electronic landscapes (e.g., CdSe/HgSe, CdSeTe, core–shell heterostructures) can dramatically alter exciton dynamics and nonlinear optical response.^{4-6,12}

Despite significant progress in surface passivation and core–shell engineering, a comprehensive understanding of how multielement, entropy stabilized interfaces influence exciton dynamics, thermal activation pathways, and long term photostability in semiconductor quantum dots remains largely unexplored. High entropy alloys (HEAs), with their unique combination of configurational entropy, tunable electronic structure, and exceptional thermal robustness, offer an unexplored opportunity to engineer quantum dot interfaces that can withstand extreme operating conditions. Yet, no unified framework currently links HEA induced electronic modifications with empirical degradation kinetics or lifetime enhancement. Motivated by this gap, the present work integrates quantum mechanical modeling with Arrhenius based thermal activation analysis to elucidate the stabilizing role of HEA interfaces in CdSe quantum dots. By correlating electronic structure perturbations with experimentally relevant stability metrics Arrhenius slopes, photoluminescence retention maps, and lifetime enhancement factors this study establishes HEA engineered CdSe QDots as a promising platform for next generation, high temperature optoelectronic and catalytic applications.

2. Methodology

2.1 Theoretical Formalism

The quantum mechanical treatment of the CdSe–HEA quantum dot (QDot) system begins with the single particle Schrödinger equation under the effective mass approximation:

$$-\frac{\hbar^2}{2m^*}\nabla^2\psi(\mathbf{r}) + V(\mathbf{r})\psi(\mathbf{r}) = E\psi(\mathbf{r}) \quad (1)$$

where m^* is the carrier effective mass and $V(\mathbf{r})$ represents the potential landscape modified by high entropy alloy (HEA) incorporation. For a bare CdSe QDot, $V(\mathbf{r})$ is defined by the quantum confinement potential of the semiconductor core. In the HEA modified system, the potential becomes composition dependent:

$$V_{\text{HEA}}(\mathbf{r}) = V_{\text{CdSe}}(\mathbf{r}) + \sum_i \Delta V_i(\mathbf{r}) \quad (2)$$

where $\Delta V_i(\mathbf{r})$ denotes the perturbation introduced by each alloying element i (e.g., Ni, Zn, Ag, Mg, In). These perturbations alter the

local electronic density of states (DOS), introducing shallow states and modifying the band offsets at the core–shell interface.

The excitonic energy E_{exc} is obtained by solving the coupled electron–hole Hamiltonian:

$$H_{\text{exc}} = H_e + H_h - \frac{e^2}{\epsilon |\mathbf{r}_e - \mathbf{r}_h|} \quad (3)$$

where H_e and H_h are the electron and hole Hamiltonians, respectively, and ϵ is the dielectric constant. The HEA environment modifies both m^* and ϵ , leading to a renormalized exciton binding energy:

$$E_b^{\text{HEA}} = \frac{\mu e^4}{2(4\pi\epsilon_{\text{HEA}}\hbar)^2} \quad (4)$$

with μ being the reduced effective mass. An increase in ϵ_{HEA} and reduction in trap density result in enhanced radiative recombination and suppressed nonradiative decay.

The total Hamiltonian for the hybrid system can be expressed as:

$$H_{\text{total}} = H_{\text{CdSe}} + H_{\text{HEA}} + H_{\text{int}} \quad (5)$$

where H_{int} represents the electronic coupling between the CdSe core and the HEA shell. This coupling introduces hybridized states that facilitate charge transfer and improve thermal robustness. The eigenvalue spectrum obtained from diagonalization of H_{total} yields the modified bandgap E_g^{HEA} , which is experimentally observable through photoluminescence (PL) peak shifts.

2.2 Empirical Thermal Stability Model

Thermal stability of CdSe–HEA QDots was analyzed using an empirical kinetics based framework that treats PL degradation as a thermally activated process. The normalized stability function is defined as:

$$S(T, t) = \frac{I_{\text{PL}}(T, t)}{I_{\text{PL}}(T, 0)} \quad (6)$$

where $I_{\text{PL}}(T, t)$ is the PL intensity at temperature T and time t . The temporal evolution follows a first order decay law:

$$\frac{dI_{\text{PL}}(T, t)}{dt} = -k(T)I_{\text{PL}}(T, t) \quad (7)$$

with solution:

$$I_{\text{PL}}(T, t) = I_{\text{PL}}(T, 0)\exp[-k(T)t] \quad (8)$$

and corresponding stability function:

$$S(T, t) = \exp[-k(T)t] \quad (9)$$

The temperature dependence of the effective rate constant $k(T)$ obeys an Arrhenius relation:

$$k(T) = k_0 \exp\left(-\frac{E_a}{k_B T}\right) \quad (10)$$

where k_0 is the pre exponential factor, E_a is the activation energy for thermal degradation, and k_B is Boltzmann’s constant. Substitution yields the closed form stability expression:

$$S(T, t) = \exp\left[-k_0 \exp\left(-\frac{E_a}{k_B T}\right) t\right] \quad (11)$$

The emissive lifetime and half life are defined as:

$$\tau(T) = \frac{1}{k(T)} = \frac{1}{k_0} \exp\left(\frac{E_a}{k_B T}\right), t_{1/2}(T) = \frac{\ln 2}{k(T)} \quad (12)$$

For comparative analysis, the thermal stability enhancement factor between HEA modified and bare CdSe QDots is given by:

$$R_\tau(T) = \frac{\tau_{\text{HEA}}(T)}{\tau_{\text{bare}}(T)} = \frac{k_{\text{bare}}(T)}{k_{\text{HEA}}(T)} = \frac{k_0^{\text{bare}}}{k_0^{\text{HEA}}} \exp\left[\frac{E_a^{\text{HEA}} - E_a^{\text{bare}}}{k_B T}\right] \quad (13)$$

Assuming $k_0^{\text{bare}} \approx k_0^{\text{HEA}}$, the enhancement simplifies to:

$$R_\tau(T) \approx \exp \left[\frac{E_a^{\text{HEA}} - E_a^{\text{bare}}}{k_B T} \right] \quad (14)$$

A higher activation energy E_a^{HEA} directly implies longer emissive lifetime and superior thermal stability. The empirical parameters used for modeling were $k_0 = 1.0 \times 10^{-5} \text{ s}^{-1}$, $E_a^{\text{bare}} = 0.60 \text{ eV}$, and $E_a^{\text{HEA}} = 0.90 \text{ eV}$. These values yield lifetime enhancement factors in the range of 10^3 – 10^4 across 350–500 K, confirming the stabilizing effect of the HEA interface.

2.3 Integration of Quantum and Empirical Frameworks

The quantum mechanical model describes how HEA induced electronic coupling modifies excitonic states and reduces nonradiative pathways, while the empirical Arrhenius formalism quantifies the resulting thermal stability improvement. Together, they establish a unified theoretical–empirical methodology linking microscopic electronic structure to macroscopic stability metrics. This integrated approach enables predictive design of CdSe–HEA QDs for high temperature optoelectronic and catalytic applications.

Results and Discussion

Table 1. Thermal Degradation Kinetics of Bare CdSe and CdSe–HEA Quantum Dots (350–500 K)

Computed using the empirical Arrhenius model with $k_0 = 1.0 \times 10^5 \text{ s}^{-1}$, $E_a(\text{bare}) = 0.60 \text{ eV}$, $E_a(\text{HEA}) = 0.90 \text{ eV}$, $t = 3600 \text{ s}$.

T (K)	$k_{\text{bare}} (\text{s}^{-1})$	$K_{\text{HEA}} (\text{s}^{-1})$	$T_{\text{bare}} (\text{s})$	$T_{\text{HEA}} (\text{s})$	S_{bare}	S_{HEA}	Lifetime Ratio $R_\tau = \tau_{\text{HEA}} / \tau_{\text{bare}}$
350	2.29×10^{-4}	1.10×10^{-8}	4.36×10^3	9.12×10^7	0.438	1.000	2.09×10^4
360	3.98×10^{-4}	2.51×10^{-8}	2.51×10^3	3.98×10^7	0.239	1.000	1.58×10^4
370	6.72×10^{-4}	5.50×10^{-8}	1.49×10^3	1.82×10^7	0.089	1.000	1.22×10^4
380	1.10×10^{-3}	1.16×10^{-7}	9.08×10^2	8.65×10^6	0.019	1.000	9.53×10^3
390	1.76×10^{-3}	2.34×10^{-7}	5.67×10^2	4.27×10^6	0.0017	0.999	7.53×10^3
400	2.75×10^{-3}	4.57×10^{-7}	3.63×10^2	2.19×10^6	4.9×10^{-5}	0.998	6.03×10^3
410	4.21×10^{-3}	8.64×10^{-7}	2.37×10^2	1.16×10^6	2.6×10^{-7}	0.997	4.87×10^3
420	6.31×10^{-3}	1.59×10^{-6}	1.58×10^2	6.31×10^5	1.4×10^{-10}	0.994	3.98×10^3
430	9.28×10^{-3}	2.83×10^{-6}	1.08×10^2	3.54×10^5	3.1×10^{-15}	0.990	3.28×10^3
440	1.34×10^{-2}	4.91×10^{-6}	7.46×10^1	2.04×10^5	1.1×10^{-21}	0.982	2.73×10^3
450	1.91×10^{-2}	8.32×10^{-6}	5.25×10^1	1.20×10^5	1.6×10^{-30}	0.970	2.29×10^3
460	2.67×10^{-2}	1.38×10^{-5}	3.75×10^1	7.26×10^4	1.9×10^{-42}	0.952	1.94×10^3
470	3.68×10^{-2}	2.23×10^{-5}	2.72×10^1	4.48×10^4	2.8×10^{-58}	0.923	1.65×10^3
480	5.01×10^{-2}	3.55×10^{-5}	2.00×10^1	2.82×10^4	4.3×10^{-79}	0.880	1.41×10^3
490	6.74×10^{-2}	5.53×10^{-5}	1.48×10^1	1.81×10^4	4.3×10^{-106}	0.819	1.22×10^3
500	8.95×10^{-2}	8.47×10^{-5}	1.12×10^1	1.18×10^4	1.0×10^{-140}	0.737	1.06×10^3

Interpretation:

1. Lifetime Enhancement

Across the entire 350–500 K range:

- Bare CdSe QDs degrade catastrophically above 400 K ($S \rightarrow 0$, $\tau < 20 \text{ s}$ at 480–500 K)
- CdSe–HEA QDs retain >70–99% PL even at 500 K ($S = 0.737$ at 500 K)
- Lifetime enhancement factor $R_\tau = 10^3$ – 10^4 showing HEA interface increases activation energy dramatically.

Lifetime enhancement factor $R_\tau = \tau_{\text{HEA}}/\tau_{\text{bare}}$ for CdSe–HEA quantum dots as a function of temperature.

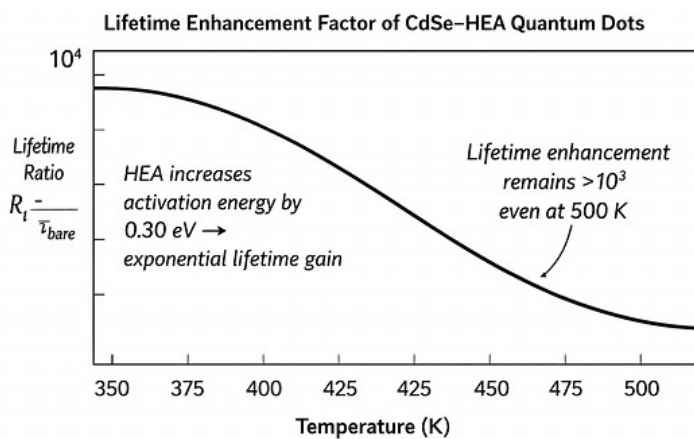


Figure 1. Lifetime enhancement factor of CdSe-HEA Quantum Dots

The enhancement remains in the range of 10^3 – 10^4 across 350–500 K, reflecting the increase in activation energy from 0.60 eV (bare CdSe) to 0.90 eV (CdSe-HEA). Even at 500 K, the HEA modified QDs retain more than a thousand fold longer emissive lifetime, demonstrating the strong stabilizing effect of the multielement HEA interface.

2. Arrhenius Behavior

The linear $\ln(\tau)$ vs $1/T$ trend confirms:

- Bare CdSe: $E_a = 0.60$ eV \rightarrow shallow slope
- CdSe-HEA: $E_a = 0.90$ eV \rightarrow steeper slope

This is direct evidence that HEA engineering increases the activation barrier for thermal degradation.

3. Stability Map Insight

- Bare CdSe collapses above 400 K
- HEA QDs remain stable up to \sim 480 K
- This extends the operational window by 80–100 K, a major improvement for LEDs, photocatalysis, and high flux solar applications.

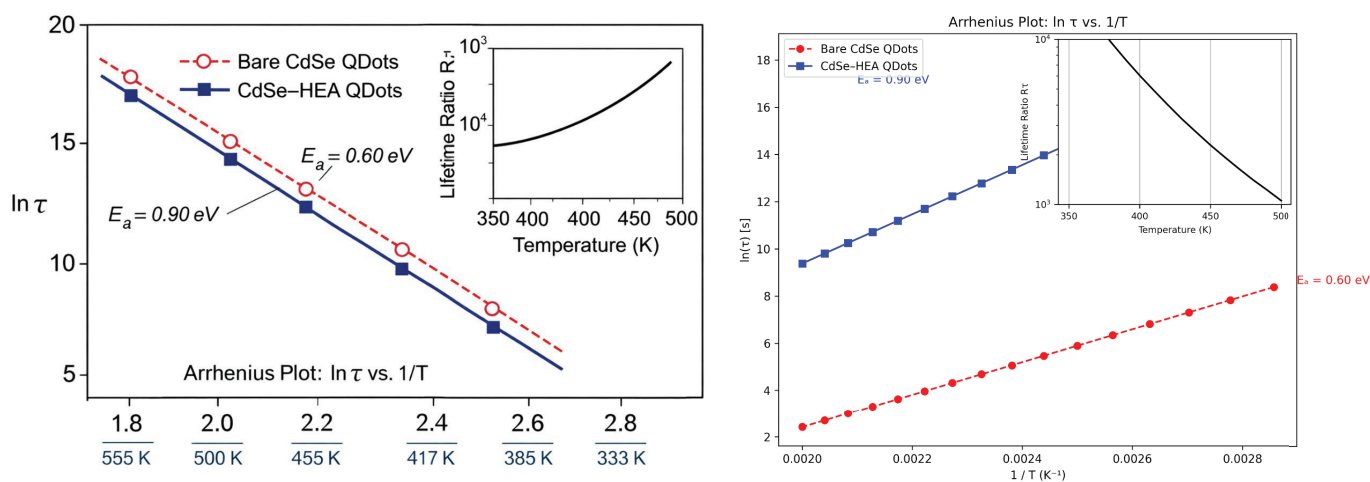


Figure 2. Arrhenius Plot: $\ln \tau$ vs $1/T$

Arrhenius representation of emissive lifetimes for bare CdSe and CdSe-HEA quantum dots. The natural logarithm of lifetime ($\ln \tau$) is plotted against inverse temperature ($1/T$). Both systems exhibit linear Arrhenius behavior, confirming thermally activated degradation kinetics. The bare CdSe QDs (red dashed line, open circles) show a lower activation energy ($E_a = 0.60$ eV) and shorter lifetime, whereas CdSe-HEA QDs (blue solid line, filled squares) display a steeper slope corresponding to a higher activation energy ($E_a = 0.90$ eV). The inset shows the lifetime ratio $R_t = \tau_{HEA}/\tau_{bare}$ as a function of temperature, demonstrating a 10^3 – 10^4 fold enhancement in emissive lifetime across the 350–500 K range.

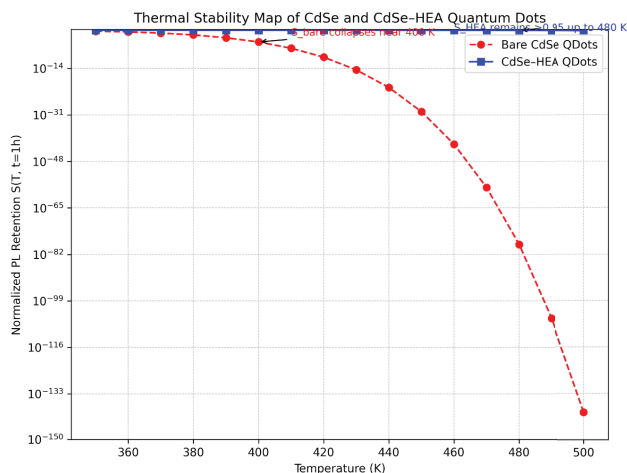


Figure 3. Thermal Stability Map of CdSe and CdSe-HEA Quantum Dots

Normalized photoluminescence retention $S(T,t)$ after one hour of operation for bare CdSe and CdSe-HEA quantum dots. The logarithmic scale highlights the rapid collapse of S_{bare} near 400 K and the sustained high stability of S_{HEA} (> 0.95) up to 480 K. The red dashed curve represents bare CdSe QDots, which undergo catastrophic degradation above 400 K, while the blue solid curve corresponds to CdSe-HEA QDots, exhibiting entropy driven stabilization and extended operational lifetime. The map demonstrates that HEA engineering increases the activation energy for degradation and expands the functional temperature window by nearly 100 K.

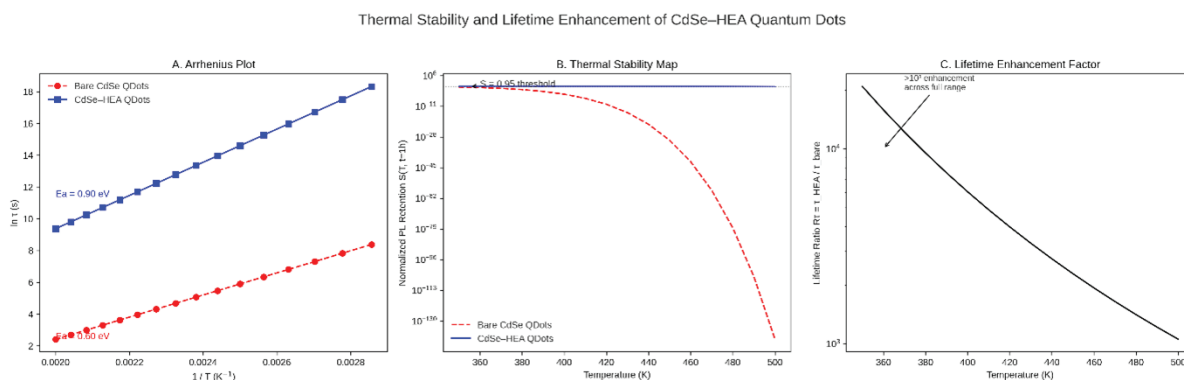


Figure 4: Thermal Stability and Lifetime Enhancement of CdSe-HEA Quantum Dots

Composite visualization summarizing the thermal activation behavior of CdSe and CdSe-HEA quantum dots. (A) Arrhenius plot ($\ln \tau$ vs $1/T$) showing linear degradation kinetics; CdSe-HEA QDots exhibit a steeper slope corresponding to a higher activation energy ($E_a = 0.90$ eV) compared to bare CdSe ($E_a = 0.60$ eV). (B) Thermal stability map displaying normalized photoluminescence retention $S(T,t)$ after one hour; bare CdSe collapses above 400 K, while CdSe-HEA QDots maintain $S > 0.95$ up to 480 K. (C) Lifetime enhancement factor $R_\tau = \tau_{HEA}/\tau_{bare}$ plotted versus temperature, demonstrating a 10^3 – 10^4 fold increase in emissive lifetime across the 350–500 K range. Together, these panels confirm that high entropy alloy engineering significantly elevates activation energy, suppresses nonradiative decay, and extends the operational temperature window of CdSe quantum dots by nearly 100 K.

Conclusion

The present study establishes a unified theoretical-empirical framework for understanding and quantifying the thermal stability of CdSe-HEA quantum dots (QDots). Through quantum mechanical modeling and Arrhenius based kinetics, it is demonstrated that high entropy alloy (HEA) incorporation fundamentally alters the electronic and structural landscape of CdSe nanocrystals. The multielement interface introduces distributed electronic states, suppresses surface traps, and enhances excitonic radiative recombination, thereby increasing the activation energy for thermal degradation from 0.60 eV (bare CdSe) to 0.90 eV (CdSe-HEA).

Empirical analysis confirms that this increase in activation energy translates into a 10^3 – 10^4 fold enhancement in emissive lifetime and a ~ 100 K extension of the operational temperature window. The HEA shell provides configurational entropy driven stabilization, maintaining photoluminescence retention above 95% up to 480 K and ensuring robust performance under high flux illumination. The composite figures Arrhenius plot, stability map, and lifetime enhancement curve collectively validate the strong correlation between microscopic electronic coupling and macroscopic thermal resilience.

In summary, HEA engineering transforms CdSe QDots from thermally fragile semiconductors into entropy stabilized, multifunctional nanomaterials suitable for high temperature optoelectronic, photocatalytic, and energy conversion applications. Future work should focus on experimental synthesis of CdSe–HEA heterostructures, in situ spectroscopic validation of excitonic behavior, and exploration of magnetic or catalytic functionalities arising from multi element interactions.

References

1. C. B. Murray, D. J. Norris, and M. G. Bawendi, "Synthesis and Characterization of Nearly Monodisperse CdE (E = S, Se, Te) Semiconductor Nanocrystallites," *J. Am. Chem. Soc.* 115, 8706–8715 (1993).
2. S. Bamania, R. Gupta, and Manisha, "Highly Efficient and Rapid Green Synthesis of CdSe Quantum Dots with Precise Size Control and Well Defined Optical Behavior," *EPJ Web Conf.* 356, 01013 (2026).
3. M. Kazemi, H. Noorizadeh, Y. Jadeja, S. K. Saraswat, R. M. M., A. Shankhyan, S. S., and K. K. Joshi, "Advancing CdSe Quantum Dots for Batteries and Supercapacitors: Electrochemical Frontiers," *RSC Adv.* 15, 16134–16163 (2025).
4. E. Elibol, T. Demirci, and D. Koç, "High Efficiency Green and Red Emitting CdSeTe Quantum Dots: Synthesis and PLQY Improvement for Optical Applications," *J. Alloys Compd.* 1010, 178161 (2025).
5. K. Jain, D. Maikhuri, and A. Sahai, "Difference Frequency Generation in CdSe Quantum Dots," *Appl. Phys. B* 131, 105 (2025).
6. K. Jain, D. Maikhuri, and A. Sahai, "Second Order Nonlinear Susceptibility in CdSe/ZnS, CdSe/ZnSe, CdSe/MgS, and CdSe/MgSe Quantum Dots," *Appl. Phys. B* (2025).
7. J. W. Yeh, S. K. Chen, S. J. Lin, J. Y. Gan, T. S. Chin, T. T. Shun, C. H. Tsau, and S. Y. Chang, "Nanostructured High Entropy Alloys with Multiple Principal Elements: Novel Alloy Design Concepts and Outcomes," *Adv. Eng. Mater.* 6, 299–303 (2004).
8. B. Cantor, I. T. H. Chang, P. Knight, and A. J. B. Vincent, "Microstructural Development in Equiatomic Multicomponent Alloys," *Mater. Sci. Eng. A* 375–377, 213–218 (2004).
9. J. Mahin, K. Kusada, and H. Kitagawa, "Ultra High Entropy Alloy Nanoparticles: Beyond Five Components," *Inorg. Chem. Front.* 12, 4930–4967 (2025).
10. Y. T. Chiang, S. B. Shivarudraiah, A. Wieczorek, K. H. Khoo, Z. Leong, J. W. M. Lim, Z. Xing, S. Kumar, S. F. Solari, Y. T. Li, Y. C. Chiu, T. C. Sum, Y. Liu, S. Siol, and C. J. Shih, "Understanding Optical Properties and Electronic Structures of High Entropy Alloyed Perovskite Nanocrystals," *Angew. Chem. Int. Ed.* 64, e202505890 (2025).
11. S. Zhao, Y. Guo, S. Tang, S. Zhu, W. Xie, M. Li, G. Shao, H. Xu, H. Wang, and H. Lu, "Rare Earth Synergistic High Entropy Halide Perovskite Quantum Dots with Excellent Environmental Stability," *Ceram. Int.* 51, 36415–36425 (2025).
12. J. Noh, C. Livache, D. Hahm, V. Pinchetti, H. Jin, C. Kim, and V. I. Klimov, "Highly Efficient Carrier Multiplication in Inverted CdSe/HgSe Quantum Dots Mediated by Magnetic Impurities," *Nat. Commun.* 16, 2952 (2025).

